Non-degenerate four-wave mixing in an optically injection-locked InAs/InP quantum dot Fabry–Perot laser

H. Huang, K. Schires, P. J. Poole, and F. Grillot

Citation: Applied Physics Letters **106**, 143501 (2015); doi: 10.1063/1.4916738
View online: http://dx.doi.org/10.1063/1.4916738
View Table of Contents: http://scitation.aip.org/content/aip/journal/apl/106/14?ver=pdfcov
Published by the AIP Publishing

Non-degenerate four-wave mixing in an optically injection-locked InAs/InP quantum dot Fabry–Perot laser

H. Huang,[1] K. Schires,[1] P. J. Poole,[2] and F. Grillot[1]
[1]*Télécom ParisTech, Ecole Nationale Supérieure des Télécommunications, CNRS LTCI, 46 rue Barrault, 75013 Paris Cedex, France*
[2]*National Research Council Canada, 1200 Montreal Road, Ottawa, Ontario K1A 0R6, Canada*

(Received 24 December 2014; accepted 23 March 2015; published online 7 April 2015)

Non-degenerate four-wave mixing in an InAs/InP quantum dot Fabry–Perot laser is investigated with an optical injection-locking scheme. Wavelength conversion is obtained for frequency detunings ranging from +2.5 THz to −3.5 THz. The normalized conversion efficiency is maintained above −40 dB between −1.5 and +0.5 THz with an optical signal-to-noise ratio above 20 dB and a maximal third-order nonlinear susceptibility normalized to material gain of 2×10^{-19} m^3/V^2. In addition, we show that injection-locking at different positions in the gain spectrum has an impact on the nonlinear conversion process and the symmetry between up- and down- converted signals.
 [http://dx.doi.org/10.1063/1.4916738]

Non-degenerate four-wave mixing (NDFWM) is a nonlinear interaction process driven by the third-order nonlinear susceptibility $\chi^{(3)}$. In semiconductor media, four-wave mixing has been extensively used to produce wavelength conversion for wavelength division multiplexed systems,[1] to balance chirping characteristics in semiconductor optical amplifiers (SOA)[2] and for the generation of high repetition rates in self-pulsating lasers through passive mode locking.[3] Stemming from the beating between the pump and probe signals, NDFWM leads to additional waves corresponding to the converted conjugate replica of the input signals. The situation where the converted signal has a frequency that is higher (resp. lower) than the pump is referred to as up- (down-) conversion. When the frequency detuning (Δf) between the pump and probe lies within a few GHz,[4] NDFWM is mostly governed by the carrier density pulsation (CDP) from which the beating between the pump and probe waves creates a dynamic grating for the gain as well as for the index. For larger frequency detunings, up to the THz range,[5] spectral hole burning (SHB) and carrier heating (CH) become the dominant mechanisms taking place within subpicosecond timescales. The former is connected to the gain saturation effects and the intraband carrier dynamics while the latter produces a beating of the carrier temperature via phonon scattering. Although values of $\chi^{(3)}$ are always higher at low frequency detunings due to the larger contribution of the CDP, the very large bandwidth offered by the SHB does remain very promising for broadband wavelength conversion.

In contrast to quantum well (QW) materials, quantum dot (QD) nanostructures exhibit a larger oscillator strength and various advantages such as an ultrafast carrier dynamics,[5,6] a wider gain spectrum,[7] higher nonlinear gain effects as well as a larger third-order nonlinear susceptibility.[8,9] In addition, due to the reduced linewidth enhancement factor (LEF, or α-factor), QD nanostructures are useful for eliminating destructive interferences among the different nonlinear processes, hence lowering the asymmetry between up- and down-converted signals.[10] Most experimental investigations of four-wave mixing have been performed on SOAs with bulk, QW and QD structures.[5,11,12] Generally, it is known that SOAs have a larger linear gain providing higher conversion efficiency, while also generating stronger amplified spontaneous emission noise, thus limiting the optical signal-to-noise ratio (OSNR).

This paper aims at extending these previous studies of SOAs, intrinsically limited by their amplified spontaneous emission noise, to semiconductor laser diodes in order to show that further improvement of the NDFWM generation and higher OSNR can be obtained. Previous investigations have been performed on both QW and QD Distributed Feedback (DFB) lasers where the lasing mode fixed by the Bragg grating was used as a pump wave, the NDFWM being enhanced by the cavity resonance.[8,13,14] Although large normalized conversion efficiencies (NCEs) have been reported with DFB structures, it has to be stressed that the corresponding nonlinear efficiency remains strongly dependent on some complex additional DFB features such as the strength of the grating coefficient, facet phase effects, or spatial hole burning, which are somewhat difficult to control from device to device.[15] In order to improve the conversion efficiency without requiring a DFB cavity, an optical injection-locking (OIL) technique is employed in this paper to select a mode of a Fabry–Perot (FP) laser and use it as pump for the NDFWM. OIL has been widely used to improve laser properties such as spectral linewidth or frequency chirp, as well as relative intensity noise and nonlinear distortion.[11,16] To this end, in our previous work, the dual OIL configuration was used for generating efficient NDWFM in a U-band InAs/InP FP laser.[17] In this work, the dual injection scheme is reemployed with a 1550 nm InAs/InP QD FP laser operating within the stable-locking range. The NCE is found to vary from −25 dB to −60 dB for frequency detunings ranging from a few tens of GHz to several THz. The locked QD FP laser thus allows efficient wavelength conversion for frequency detunings much larger than those reached for similar QD SOAs.[12]

The device studied was an InAs/InP QD laser grown on a (001) oriented n-type InP substrate.[18] An n-type cladding was first grown, followed by a 350 nm thick 1.15Q

waveguiding core containing the 5 layers of QDs in the centre. The dot density per layer was around $3.5 \times 10^{10}\,\mathrm{cm}^{-2}$. An upper p-type InP cladding layer was then grown (containing an etch stop for ridge fabrication) followed by a heavily doped p-type InGaAs contact layer. Single mode ridge waveguide lasers with 3 μm wide ridges were then fabricated, cleaved to make 1 mm long devices, and mounted for testing at a temperature of 293 K. The measured device had a threshold current of $I_{th} = 39$ mA corresponding to a threshold current density injected into the active area of 1.3 kA/cm^2. The gain spectrum of the device was measured using the Hakki-Paoli method.[17] Fig. 1 shows the gain spectra for various pump currents ranging from 0.64 to 1.0 times I_{th}. At the gain peak (1543 nm), the threshold net modal gain was found to be of 11 cm^{-1}. The below-threshold LEF is then calculated from the wavelength shift and gain change with respect to the current increase following the relationship

$$\alpha = -\frac{4n\pi}{\lambda^2}\frac{\Delta\lambda/\Delta I}{\Delta g/\Delta I}, \tag{1}$$

with n the effective group index, λ the photon wavelength, and g the net modal gain. Since the measurements are done under continuous wave condition, the wavelength shift caused by thermal effects must be taken into account. To this end, the wavelength red-shift due to thermal effects, measured by varying the pump current right above threshold, is subtracted from the wavelength blue-shift measured below threshold.[19] The inset of Fig. 1 represents the evolution of the LEF as a function of the lasing wavelength. After elimination of the thermal effects, the LEF spectrum is found to range from 1.3 to 4.6 with a value of 2.4 at the gain peak.

Fig. 2 shows the OIL experimental setup used for the NDFWM experiments. The light from two external tunable lasers, TL1 and TL2, are combined using an 80/20 coupler and injected into the slave FP laser through an optical circulator. TL1 is used as master laser in order to lock one of the FP modes, which allows selecting which mode will be used as pump for the wave mixing. TL2 is then used as probe to generate the four-wave mixing with the locked FP mode. A lens-ended fiber was used to both inject the light from TL1 and TL2 into the slave laser and collect the light emitted by

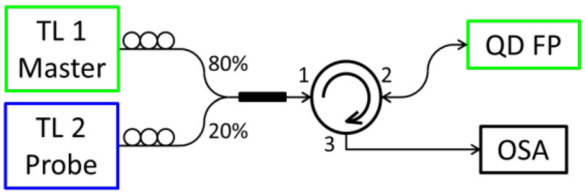

FIG. 2. Optical injection-locking (OIL) setup used for the NDFWM experiments. TL1 is the master laser used to lock a given FP mode. TL2 is then used as probe to generate the four-wave mixing in the semiconductor material.

the latter. In what follows, the QD laser is biased at $2.5 \times I_{th}$. The optical injection-locking frequency detuning Δf_{OIL}, defined as the frequency difference between TL1 and the solitary targeted FP mode, is fixed to -11 GHz, for which a relatively low injection ratio of -3 dB is sufficient to lock the target mode. The optical power of the probe signal is maintained at 450 μW (measured at port 2 of the circulator) and is monitored during the whole experiment.

TL2 is then injected into the locked slave laser in order to produce the wave mixing. The NDFWM detuning Δf, defined as the frequency detuning between TL2 and the locked mode and equivalent to the detuning between TL2 and TL1, is then varied in such a way that TL2 always coincides with one of the suppressed FP cavity mode in order to obtain maximum conversion. The optical spectrum at the output of the slave laser is then measured using an optical spectrum analyzer (OSA) with a 10 pm resolution.

Fig. 3 shows a typical NDFWM spectrum recorded for down conversion with $\Delta f = 150$ GHz when locking a mode at the gain peak to use it as pump wave. The green peak (pump) represents the FP mode locked at the frequency of TL1, and the side-modes in black correspond to well-suppressed modes of the FP laser. The blue peak is the probe wave, at the frequency of TL2, and the red peak—the converted signal stemming from the beating between the pump and probe waves.

The NCE, in mW^{-2}, is expressed as[17]

$$\eta_{NCE} = \frac{P_{converted\ signal}}{P_{pump}^2 P_{probe}}. \tag{2}$$

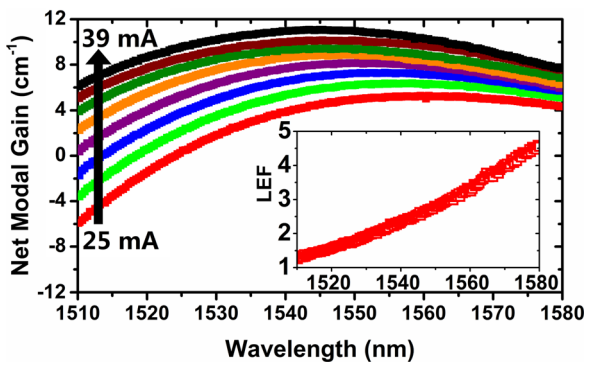

FIG. 1. Measured net modal gain as a function of the lasing wavelength for different pump currents (step: 2 mA); the figure in inset represents the below-threshold linewidth enhancement factor (LEF) as a function of the lasing wavelength.

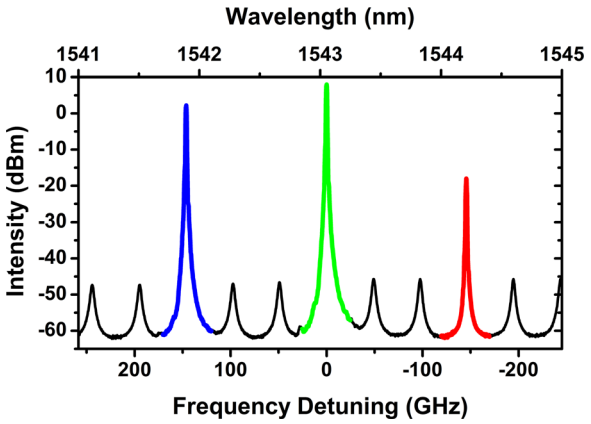

FIG. 3. Measured NDFWM optical spectrum for down-conversion with $\Delta f = 150$ GHz.

The optical powers are defined after propagation within the active region. Experimentally, these powers are usually approximated by using the peak powers in the measured optical spectra. When expressed in logarithmic scale, the values given in dB in this paper correspond to $10 \times \log_{10}$ (η_{NCE}/1mW^{-2}). As the NCE is not a mere ratio of the measured powers, it is of prime importance to properly estimate the losses introduced by the setup from the facet of the laser to the input of the OSA, so as not to over-estimate the value of the NCE. The setup losses were measured using a free-space measurement of the power at the output of the free-running slave laser and a measurement of the power reaching the input of the OSA, and the value of P_{pump} was corrected accordingly.

Fig. 4(a) presents the NCE as a function of the absolute value of the pump-probe detuning Δf, when using a mode at the gain peak as pump wave. Up- (respectively, down-) conversion is shown in red with square markers (blue with triangle markers). As previously reported,[5,11] the conversion efficiency is found to be higher when the CDP mechanism occurs with a maximum value of about −25 dB for a frequency difference of a few GHz. Overall, the NCE is found above −45 dB (horizontal dashed line in Fig. 4(a)) until 500 GHz for down-conversion and 1.5 THz for up-conversion. At larger pump-probe detunings, SHB and CH dominate allowing conversion up to detunings as large as 3.5 THz in the case of up-conversion, but at the price of an NCE that does not exceed −60 dB. Fig. 4(b) gives the corresponding OSNR, which is defined as the peak power ratio between the converted signal and the nearest side modes. As before, up- (respectively, down-) conversion is shown in red with square markers (blue with triangle markers). A high optical SNR, larger than 20 dB, is maintained up to 500 GHz for down-conversion and up to 1.5 THz for up-conversion. Under frequency detunings above 2 THz, the converted signal is however found to sink down to the noise level leading to an OSNR close to 1 dB both for up- and down-conversion. Compared to similar InAs/InP nanostructured SOAs, these results show a larger OSNR and the achievement of conversion for NDFWM frequency detunings further into the THz range, without the need of using long interaction lengths.[12] Overall, Fig. 4 also reveals a reduced asymmetry between up- and down-conversion profiles. Owing to a reduced LEF measured on this InAs/InP QD laser, a lower phase between nonlinear processes (CDP and SHB) can lead to a constructive interference of these effects and to a nonlinear conversion less dependent on the sign of the detuning, as shown in Fig. 4(a). Let us note that the down-converted signal still decays slightly faster than the up-converted one since the former experiences a larger LEF as reported in Fig. 1. The impact of the pump wavelength on the conversion efficiency is also investigated by locking a mode ±5 nm from the gain peak, namely, at 1538 and 1548 nm. The optical injection-locking conditions are kept the same as when locking the mode at the gain peak. Fig. 5 shows the measured (a) up- and (b) down-conversion NCE as a function of the frequency detuning and for the three pump wavelength conditions that are 1538, 1543, and 1548 nm.

It can be seen that when using a probe of shorter wavelength, the values of the NCE increase for down-conversion and decrease for up-conversion. For a detuning of 1 THz, the difference between the NCE measured for up- and down-conversion is thus found to be of 5 dB when using a mode at 1538 nm as pump, against 13 dB when using a mode at 1548 nm as pump. Fig. 1 shows that the LEF at 1538 and 1548 nm is of 2.2 and 2.7, respectively, and a lower value of the LEF can indeed contribute to a lower asymmetry

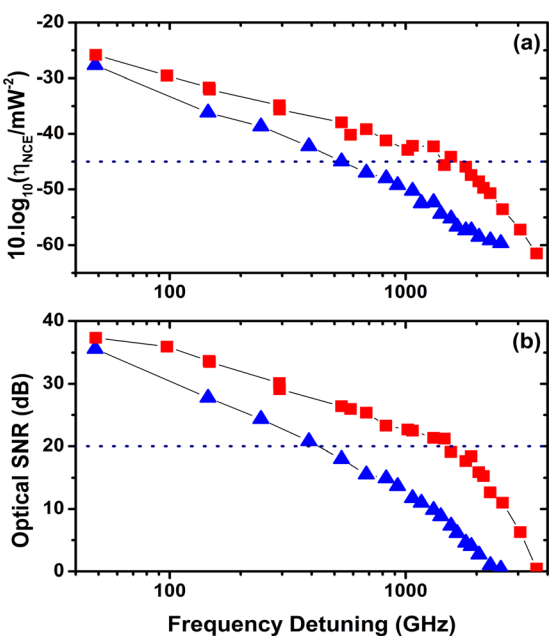

FIG. 4. Measured NCE (a) and OSNR (b) as a function of the pump-probe frequency detuning, when locking a mode of the slave FP at the gain peak. The up- and down-conversion signals are represented by red squares and blue triangles, respectively.

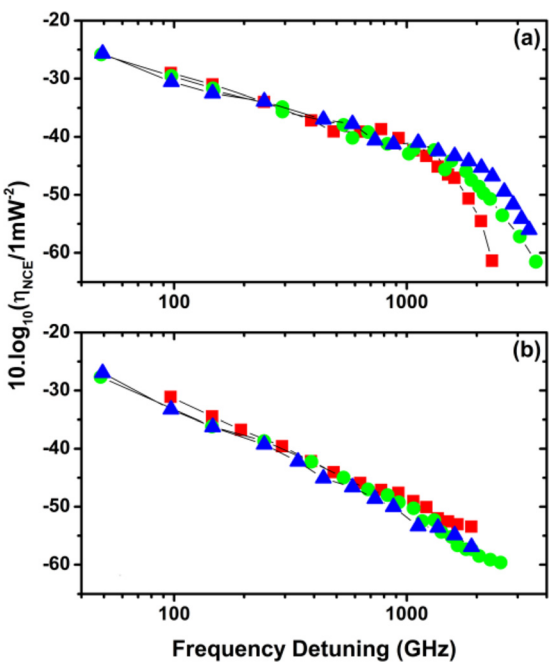

FIG. 5. Experimental NCE for different injected pump wavelengths for (a) up conversion and (b) down conversion. The red, green, and blue colors represent, respectively, the results obtained when locking the pump mode at 1538, 1543, and 1548 nm, respectively.

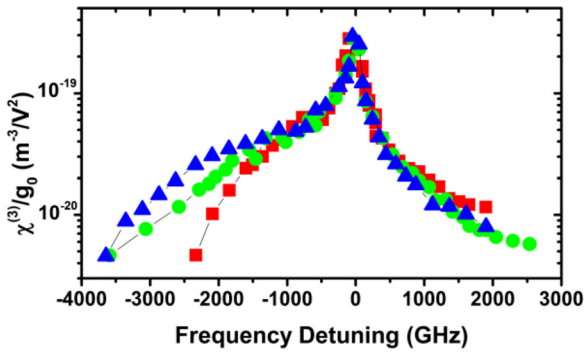

FIG. 6. The normalized susceptibility $\chi^{(3)}/g_0$ with the frequency detuning for different injected pump wavelengths. The red squares, green circles, and blue triangles represent the results obtained when locking the pump mode at 1538, 1543, and 1548 nm, respectively.

between up- and down- conversion.[11] The shape of the gain spectrum must also be taken into account: in the case of up-conversion for a pump at 1548 nm, the converted signal has a wavelength lower than that of the pump and thus lies around the peak of the gain spectrum. On the contrary, in the case of up-conversion for a pump at 1538 nm, the converted signal experiences a much lower gain.

The measurements of the NCE allow extraction of the third-order nonlinear susceptibility $\chi^{(3)}$ of the gain medium. To estimate the nonlinear susceptibility, a traveling-wave model can be used to describe the propagation of the NDFWM conjugate beam inside a semiconductor laser:[8,20]

$$\eta_{NCE} = \left|\frac{E_{conv}}{E_{pump}^2 E_{probe}}\right|^2 = \left|\frac{3k_0}{4n}\Gamma\chi^{(3)}\frac{\exp\left(\frac{\Gamma g L}{2}\right)-1}{\Gamma g}\right|^2, \quad (3)$$

where E_{conv}, E_{probe}, and E_{pump} are the field amplitudes of the converted signal, probe, and pump waves, respectively, while k_0 is the wave vector of the conjugate light in vacuum, n the refractive index, Γ the optical confinement factor, g the net material gain of the active region, and L the cavity length of the FP laser. Based on Eq. (2), the expression of $\chi^{(3)}$ normalized to the net material gain at threshold g_0 is extracted for each measured converted signal.

Fig. 6 represents $\chi^{(3)}/g_0$ as a function of the frequency detuning for different injected pump wavelengths. In the short detuning range, $\chi^{(3)}/g_0$ is enhanced due to the stronger beating between the pump and probe, while at larger detunings, $\chi^{(3)}/g_0$ is reduced following the same trend as the NCE in Fig. 5 (a). The maximum value under zero frequency detuning is around 2×10^{-19} m^3/V^2, which is slightly higher than the values reported for InAs/GaAs QD DFB.[7]

To conclude, this paper reports a comprehensive NDFWM study in an InAs/InP QD FP laser, employing an optical injection-locking technique. Taking advantage of the SHB and CH—both driven by fast carrier-carrier and carrier-phonon scatterings, results show that a laser cavity allows extending the detuning range in the THz window up to −3.5 THz, as well as maintaining an NCE beyond −40 dB up to −1.5 THz with a large OSNR above 20 dB. The level of nonlinear conversion is found to be more efficient than the one obtained on QD SOAs grown on the same material system with a maximum $\chi^{(3)}/g_0$ of 2×10^{-19} m^3/V^2. In addition, results prove that injection-locking different modes at different positions in the gain spectrum has a strong effect on the conversion efficiency and on the asymmetry between up- and down-converted signals. Further work will now concentrate on the analysis of the transmission capabilities of the converted signals as well as on the nonlinear conversion efficiency provided by the excited level of QD nanostructures.

This work was supported by Institut Mines Télécom (IMT) through the Futur & Ruptures program and by the French National research Agency (ANR) through the Nanodesign Project funded by the IDEX Paris-Saclay, ANR-11-IDEX-0003-02.

[1]D. D. Marcena, D. Nesset, A. E. Kelly, M. Brierley, A. D. Ellis, D. G. Moodie, and C. W. Ford, Electron. Lett. **33**, 879–880 (1997).[C]
[2]H. Soto and D. Erasme, Appl. Phys. Lett. **68**, 3698 (1996).
[3]J. Renaudier, G. H. Duan, J. G. Provost, H. Debregeas-Sillard, and P. Gallion, IEEE Photonics Technol. Lett. **17**, 741–743 (2005).
[4]G. P. Agrawal, J. Opt. Soc. Am. B **5**, 147–159 (1988).
[5]D. Nielsen and S. L. Chuang, Phys. Rev. B **81**, 035305 (2010).
[6]A. J. Zilkie, J. Meier, M. Mojahedi, P. J. Poole, P. Barrios, D. Poitras, T. J. Rotter, C. Yang, A. Stintz, K. J. Malloy, P. W. E. Smith, and J. S. Aitchison, IEEE J. Quantum Electron. **43**, 982–991 (2007).
[7]H. Li, G. T. Liu, P. M. Varangis, T. C. Newell, A. Stintz, B. Fuchs, K. J. Malloy, and L. F. Lester, IEEE Photon. Technol. Lett. **12**, 759–761 (2000).
[8]H. Su, H. Li, L. Zhang, Z. Zou, A. L. Gray, R. Wang, P. M. Varangis, and L. F. Lester, IEEE Photonics Technol. Lett. **17**, 1686–1688 (2005).
[9]T. Akiyama, O. Wada, H. Kuwatsuka, T. Simoyama, Y. Nakata, K. Mukai, M. Sugawara, and H. Ishikawa, Appl. Phys. Lett. **77**, 1753–1755 (2000).
[10]T. Akiyama, H. Kuwatsuka, N. Hatori, Y. Nakata, H. Ebe, and M. Sugawara, IEEE Photonics Technol. Lett. **14**, 1139–1141 (2002).
[11]C. H. Lee, *Microwave Photonics* (CRC Press, 2007).
[12]Z. G. Lu, J. R. Liu, S. Raymond, P. J. Poole, P. J. Barrios, D. Poitras, F. G. Sun, G. Pakulski, P. J. Bock, and T. Hall, Electron. Lett. **42**, 1112–1113 (2006).
[13]A. Mecozzi, A. D'Ottavi, and R. Q. Hui, IEEE J. Quantum Electron. **29**, 1477–1487 (1993).
[14]T. Simoyama, H. Kuwatsuka, and H. Ishikawa, Fujitsu Sci. Tech. J. **34**, 235–244 (1998).
[15]F. Grillot, G. H. Duan, and B. Thedrez, IEEE J. Quantum Electron. **40**, 231–240 (2004).
[16]T. B. Simpson, J. M. Liu, and A. Gavrielides, IEEE Photonics Technol. Lett. **7**, 709–711 (1995).
[17]C. Wang, F. Grillot, F. Y. Lin, I. Aldaya, T. Batte, C. Gosset, E. Decerle, and J. Even, IEEE Photon. J. **6**, 1500408 (2014).
[18]P. J. Poole, K. Kaminska, P. Barrios, Z. Lu, and J. Liu, J. Cryst. Growth **311**, 1482–1486 (2009).
[19]B. Zhao, T. R. Chen, S. Wu, Y. H. Zhuang, Y. Yamada, and A. Yariv, Appl. Phys. Lett. **62**, 1591 (1993).
[20]H. Kuwatsuka, H. Shoji, M. Matsuda, and H. Ishikawa, IEEE J. Quant. Electron. **33**(11), 2002–2010 (1997).